J. Phys. B: At. Mol. Opt. Phys. **23** (1990) 3839-3847. Printed in the UK

Coincident charge state production in F^{6+} + Ne collisions

D R Schultz†, R E Olson†, C O Reinhold†, S Kelbch‡, C Kelbch‡, H Schmidt-Böcking‡ and J Ullrich§

† Department of Physics and Laboratory for Atomic and Molecular Research, University of Missouri-Rolla, Rolla, MO, USA

‡ Institut für Kernphysik, Universität Frankfurt, D-6000 Frankfurt-am-Main 90, Federal Republic of Germany

§ Gesellschaft für Schwerionenforschung, D-6100 Darmstadt, Federal Republic of Germany

Received 12 June 1990, in final form 10 August 1990

Abstract. Total cross sections are presented for the production of various stages of multiple ionization of the target in coincidence with the final projectile charge state for collisions of F^{6+} with Ne at 10 and 15 MeV. In particular, the current measurements are compared with the results of a new classical trajectory Monte Carlo method in which electrons are included explicitly on both target and projectile (*n*CTMC) and with those based on the conventional independent electron model (IEM). It is shown by the good agreement with experiment that the *n*CTMC model simultaneously represents well the ionization, charge transfer and excitation channels for both target and projectile. Further, it is demonstrated that the IEM is in clear disagreement with the present experiment and is inadequate to predict the outcome of such multi-electronic transition processes. However, the IEM is shown to provide a reasonable estimate of the free electron production, that is, the cross section summed over charge states weighted by the number of electrons liberated. The IEM is also used to illustrate a process in cusp electron production where electrons are interchanged between the target and projectile.

1. Introduction

The study of the final charge states of both the target and projectile in coincidence after a highly energetic collision is a relatively new tool that may be used to probe the interaction of multiply charged ions and atoms. In fact, in these collisions, the kinetic energy available greatly exceeds the sum of the binding energies of the electrons present and, consequently, many-electron transitions such as multiple ionization and capture to and from the projectile and target may readily occur. Experimentally, measurements of these processes rely on the detection and time correlation of two ions, and yield detailed information as to stripping of, and capture to, the projectile in coincidence with the charge state of the recoil target ion. From a theoretical point of view, study of these coincident charge state production cross sections presents a challenge in that the various stages of ionization, capture and excitation must be well represented for both the projectile and target simultaneously in a detailed many-body problem.

Here we present new theoretical and experimental determinations of the coincident charge state production cross sections for 10 and 15 MeV F^{6+} ions colliding with Ne. Experimentally, total cross sections for the production of $F^{(6-i)+}$ ($i = -1, 0, 1, 2$) projectile ions in coincidence with Ne^{j+} ($j = 1$-8) recoil ions have been determined; that is, for the reactions

$$F^{6+} + Ne \rightarrow F^{(6-i)+} + Ne^{j+} + (j-i)\,e. \tag{1}$$

0953-4075/90/213839+09$03.50

The theoretical treatment utilized is the first application of the *n*-explicit electron classical trajectory Monte Carlo (*n*CTMC) technique in which electrons have been included on the projectile in addition to those on the target. We also include a treatment based on the conventional independent electron model (IEM) for comparison and in order to study the free electron production doubly differential cross section. It is expected that the *n*CTMC model should be an improvement over the IEM since it takes into account (i) the variations in the sequential ionization potentials of the target, (ii) the projectile-electron–target-electron interactions and (iii) the final state autoionization of the target. That is, such a model in which the multielectronic transitions are represented more fully than in the IEM should be required to provide a complete description of the coincident charge state distributions.

Also, an interesting probe of the dynamics of the ionization process has been the study of the peak in the distribution of electrons ejected with velocities near that of the projectile. In particular it is usually assumed that at small forward angles this peak is composed of electrons ejected from the target in the process of 'electron capture to the continuum' (ECC) and electrons ejected from the projectile in 'electron loss to the continuum' (ELC). These processes are important in the present context in that their discrimination requires the coincident detection of the final projectile charge. We describe below a process in which electrons are interchanged between target and projectile leaving the projectile charge unchanged and which also contribute to the peak formation.

Many of the previous measurements of coincident charge state processes have investigated the production of slow highly charged recoil ions as an alternative to complex ion sources (see, for example, Cocke 1979, Gray *et al* 1980, Schlachter *et al* 1982, Kelbch *et al* 1985, Ullrich *et al* 1986) and, as well, studies were carried out to explore the behaviour with impact energy and physical mechanisms underlying (e.g. Müller *et al* 1986) multiple ionization. In addition, a number of works have been performed observing coincidence between recoil ion charge state and projectile energy loss and scattering angle (Schuch *et al* 1988, Kelbch *et al* 1988), recoil-ion energy (Olson *et al* 1987) and various differential cross sections (Olson *et al* 1989). Quite recently, coincident charge state measurements have been reported by Tawara *et al* (1990) for Ne ions on Ne, by Datz *et al* (1990) for I and U ions on He and by Freyou *et al* (1990) for O and C ions on Ne in triple coincidence with cusp electrons.

2. Experimental technique

The present total cross section measurements have been accompanied by determinations of differential cross sections, the results of which have been presented elsewhere (Kelbch *et al* 1990) along with a detailed description of the experimental set-up. In brief, the charge state analysed F^{6+} beam from the FN-tandem accelerator of the University of Aarhus was collimated and passed through the target region containing Ne at low pressure. Having passed this differentially pumped gas target cell, the projectiles were magnetically charge state analysed and detected simultaneously by a one-dimensional position sensitive channel-plate (CP) detector. The recoil ions produced in the target cell at a pressure less than 8.0×10^{-4} Torr were extracted out of the reaction volume by an electric field of about 500 V cm^{-1}. They drifted through a field-free tube to focus in time, and were then detected by another CP detector. A coincidence between the scattered projectiles and the recoil ions enables the separation

of the recoil ion charge states due to their different time-of-flights in the extraction field and the drift tube. The time resolution of about 6 ns was sufficient to clearly identify all Ne recoil ion charge states up to Ne^{8+}.

Setting windows on the different final charge states of the projectile, $(6-i)$, recoil time-of-flight spectra for each specific channel were generated. Integration of the true coincidences for each recoil ion state, j, yields relative cross sections, $\sigma'(6-i,j)$. Since recoil ions and projectiles for all i and j were measured simultaneously, the cross sections are inherently normalized relative to each other within statistical errors. Therefore, it was sufficient for the absolute normalization of all the cross sections to measure the total single capture cross section,

$$\sigma(6-1) = \sum_{j=1}^{N} \sigma'(6-1,j). \tag{2}$$

In a separate experiment the ratio of the charge exchanged projectiles was measured under single collision conditions as a function of the target pressure between 10^{-5} and 10^{-3} Torr. Knowing the length of the target cell and the pressure inside, total charge transfer cross sections were obtained. In that experiment a position-sensitive parallel-plate avalanche detector was used to determine all final projectile charge states simultaneously including the fraction of the beam which did not undergo a charge exchange reaction. The total errors of the cross sections presented are below 25% and are due to the uncertainties in the determination of the effective target length (20%) and the absolute pressure (5%).

3. Theoretical method

The results of these measurements have been compared with those obtained with an extension of the n-electron classical trajectory Monte Carlo (nCTMC) method (Olson 1988, Olson *et al* 1989). This method was originally introduced to simulate an ion-atom collision in which the projectile was treated as a fully stripped core impinging upon a target of a core and n active electrons. Each electron in the initial state of the target is bound by an amount given by the proper experimentally determined sequential ionization potential, and their phase-space distributions are microcanonical (cf Abrines and Percival 1966). The projectile-electron interactions are Coulombic and the target-core-electron interactions are given by static screened Coulomb potentials, the screening taking partial account of the electron-electron interactions. At the impact velocities considered, the K-shell electrons of neon may be considered inactive.

Here we extend this method by explicitly including an electron on the projectile so as to be able to model the effects of stripping of the projectile and the interaction during the collision of the projectile electron with the target electrons. Therefore, the F^{6+} ion is represented as a non-active K-shell and one active electron. Its binding energy is also given by the experimental ionization potential and it interacts with its core through a screened Coulomb potential and through unscreened Coulomb potentials with the target core and electrons. Its phase-space distribution is given as well by the microcanonical distribution. Finally, since in the collision target inner-shell vacancies or doubly excited states may occur, we approximate, as described by Olson *et al* (1989), the autoionization of Ne and electron indistinguishability subsequent to the collision.

For comparison with this n-body calculation, we have also performed calculations using a three-body treatment and the independent electron model. Specifically, we perform two three-body CTMC calculations, one for electron removal from the target and one for electron removal from the projectile, and then combine the resulting probabilities to obtain coincident charge state information. In the first step, the F^{6+} projectile impinges on Ne containing one active electron. To this three-body result the IEM (cf McGuire and Weaver 1977) is applied to simulate electron removal from the full eight-active electron target. The active electron is bound by the first ionization potential of neon and interacts with both the neon core and the projectile through Hartree-Fock model potentials which simulate the effects of the screening produced by the other electrons (see Reinhold *et al* (1990) for a full description of this model applied to a different system). The probability for m-fold loss by capture to a projectile and n-fold ionization of the target is given by

$$P^{\mathrm{Ne}}_{m,n}(b) = \binom{N}{N-m}\binom{N-m}{N-m-n}\tilde{P}^{m}_{\mathrm{c}}(b)\tilde{P}^{n}_{\mathrm{i}}(b)[1-\tilde{P}_{\mathrm{c}}(b)-\tilde{P}_{\mathrm{i}}(b)]^{N-m-n} \tag{3}$$

where $\tilde{P}_{\mathrm{c}}(b)$ and $\tilde{P}_{\mathrm{i}}(b)$ are the one-electron probabilities for charge transfer and ionization and N is the total number of electrons. In the second step, the active electron is placed on the projectile so as to obtain the probabilities of stripping. In this case the electron again interacts with the projectile and target core through model potentials. In particular, the coincident charge state probabilities may then be obtained by summing over all processes that result in a particular pair of final charge states. That is, the probability of obtaining a projectile charge state of $(6-i)$ in coincidence with a target charge state (j) is

$$\mathscr{P}_{6-i,j}(b) = \sum_{\substack{m,n \\ m',n'}} P^{\mathrm{F}^{6+}}_{m',n'}(b)P^{\mathrm{Ne}}_{m,n}(b) \tag{4}$$

where the sum extends subject to the number of electrons each centre has to give up (i.e. $0 \leqslant m'+n' \leqslant 1$, $0 \leqslant m+n \leqslant 8$) and where the m'- and m-fold charge transfers and n- and n'-fold ionizations add to $i = m-m'-n'$ and $j = m+n-m'$. The total cross sections are then given by

$$\sigma[6,0;(6-i),j] = 2\pi \int \mathscr{P}_{6-i,j}(b)b\,\mathrm{d}b \tag{5}$$

where the notation $[6,0;(6-i),j]$ indicates the projectile and target, initial and final charge states.

4. Results and discussion

The results of both our experimental and theoretical investigations are presented in figures 1 and 2 for 10 and 15 MeV F^{6+} impact, respectively. In part (a) of each of these figures we present the cross section for the production of various charge states of Ne in coincidence with single ionization of F^{6+}. As the data indicate, when the projectile is stripped of its outer electron, the largest probability occurs for the simultaneous loss of three electrons from the target. In contrast, as displayed in 1(b) and 2(b), when the projectile charge is left unchanged in the collision, the largest cross section is for the

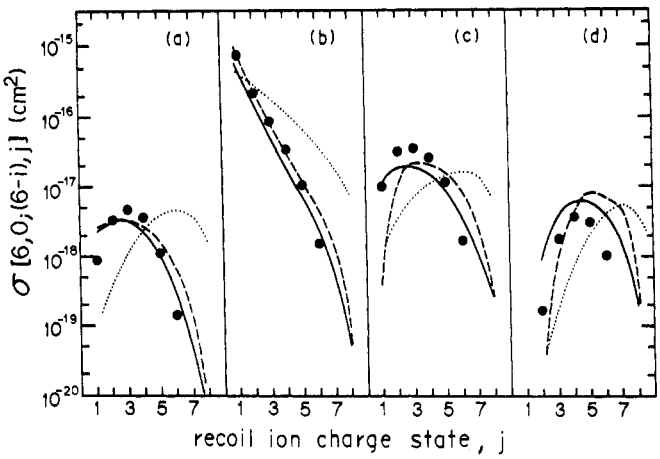

Figure 1. Coincident charge state total cross sections for 10 MeV $F^{6+} + Ne \rightarrow F^{(6-i)+} + Ne^{j+}$: squares, present experiment; full curve, *n*CTMC without autoionization; broken curves, *n*CTMC with autoionization; dotted curve, independent particle model CTMC. (a) Single ionization of F^{6+} in coincidence with multiple ionization of Ne. (b) Multiple ionization of Ne. (c) Single capture to F^{6+} in coincidence with multiple ionization of Ne. (d) Double capture to F^{6+} in coincidence with multiple ionization of Ne.

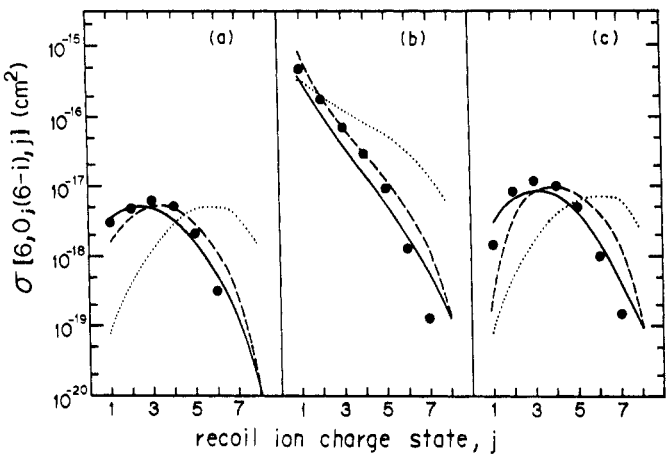

Figure 2. Same as figure 1 for 15 MeV $F^{6+} + Ne \rightarrow F^{(6-i)+} + Ne^{j+}$.

single ionization of Ne. However, as indicated in 1(c), 2(c) and 1(d) for the 10 MeV case, for single and double capture to the projectile, the dominant channel is for the simultaneous production of Ne^{3+}. We note the generally excellent agreement of the *n*CTMC results with the measurements and that the IEM results do not reproduce well the coincident charge state production cross sections.

The behaviour of the cross sections when the projectile charge does not change is such that the number of electrons removed is in approximate inverse proportion to the sequential ionization potentials of the target and therefore single ionization is largest, followed by double ionization, triple ionization, etc. However, when the projectile either gains or loses electrons, the monotonic decrease of the cross section with increasing recoil ion charge is dramatically changed. This trend is a consequence

of the fact that the impact parameter dependence of multiple ionization of Ne strongly overlaps with the range of the ionization and charge transfer for F^{6+}.

In particular, since the active electron in F^{6+} is relatively deeply bound and occupies a rather tight orbit, the ionization probability drops off quickly and has only a small impact parameter range (i.e. at 10 MeV, the removal probability is down to 10% at 1.4 au). Similarly, due to its large charge, capture to F^{6+} is dominated by small impact parameter collisions. For Ne, in contrast, single ionization requires a rather soft, large impact parameter collision, and multiple ionization dominates at small impact parameters. The result is that for the small impact parameter collisions which produce a charge change of the F^{6+}, the largest overlap is with the multiple ionization probability. Thus, when the projectile charge is changed, single ionization is less likely than multiple ionization, accounting for the initial rise with recoil charge state of the cross section. The subsequent drop reflects the diminished probability of reaching the highest levels of ionization of Ne due to the higher binding of the inner electrons. This picture obtained here is consistent with the explanation put forth by Ullrich *et al* (1986).

As is well known, the IEM overestimates the higher stages of ionization, as illustrated in figures 1(b) and 2(b). In addition, since in this model the capture process from Ne is represented only by a single binding energy whereas capture is quite sensitive to velocity matching, the capture cross section is greatly underestimated. However, as indicated in tables 1 and 2, the total cross section for free electron production (found by multiplying the cross section for each stage of ionization by the number of electrons liberated and summing) in the IEM does provide a reasonable estimate. That is, the

Table 1. Free electron production cross sections (in cm^2) for 10 MeV F^{6+} + Ne collisions comparing theory and experiment. (a) and (b) indicate the results without and with autoionization, respectively.

Process: $F^{6+}+Ne\rightarrow$	Experiment	*n*CTMC (a)	*n*CTMC (b)	IEM
$F^{7+}+Ne^{j+}$	8.7 (−17)	3.5 (−17)	4.3 (−17)	1.0 (−16)
$F^{6+}+Ne^{j+}$	1.6 (−15)	1.0 (−15)	2.0 (−15)	3.1 (−15)
$F^{5+}+Ne^{j+}$	5.3 (−16)	2.7 (−16)	3.5 (−16)	3.8 (−16)
$F^{4+}+Ne^{j+}$	1.0 (−16)	1.1 (−16)	1.3 (−16)	9.9 (−17)
Sum	2.3 (−15)	1.4 (−15)	2.5 (−15)	3.7 (−15)

Table 2. Free electron production cross sections (in cm^2) for 15 MeV F^{6+} + Ne collisions comparing theory and experiment. (a) and (b) indicate the results without and with autoionization, respectively.

Process: $F^{6+}+Ne\rightarrow$	Experiment	*n*CTMC (a)	*n*CTMC (b)	IEM
$F^{7+}+Ne^{j+}$	8.1 (−17)	5.9 (−17)	7.1 (−17)	1.1 (−16)
$F^{6+}+Ne^{j+}$	1.2 (−15)	8.2 (−16)	1.9 (−15)	3.4 (−15)
$F^{5+}+Ne^{j+}$	1.3 (−16)	1.2 (−16)	1.5 (−16)	1.5 (−16)
Sum	1.4 (−15)	1.0 (−15)	2.1 (−15)	3.7 (−15)

calculated free electron production cross section does not disagree with experiment as much as does the cross section for production of the highest charge states alone. Thus, if one is only interested in the gross electron production cross sections, rather than the specific coincident charge states, the IEM treatment which we have used provides a reasonable approximation.

Inspection of the *n*CTMC results as well as IEM probabilities indicates that even at this relatively large collision velocity (10 MeV F^{6+} corresponds to a velocity of 4.6 au), processes in which electrons change centre are significant. That is, it is possible, for example, that an electron originally bound to the target would take the place of the projectile electron, which in turn would be removed. The net effect of this process is that the projectile charge does not change even though it was the projectile electron which was removed. Higher order interchange was also observed as in the case where a target electron was captured by the projectile and simultaneously the projectile electron was captured by the multiply ionized recoil ion.

One would not expect that these interchanges would be observable experimentally because of the indistinguishability of the electrons. However, we would like to point out that interchange should significantly affect attempts to analyse the ECC and ELC cusps in the ejected electron spectra at collision velocities where the probability of capture to the projectile along with an associated ionization of the projectile is large. Conventionally, the discrimination between ECC and ELC has been made by measuring the doubly differential cross sections for the production of free electrons in the vicinity of ejected electron energies corresponding to equivelocity with the projectile, in coincidence with the final charge state of the projectile. If the cusp was found to be produced in coincidence with no charge change of the projectile, it was assumed that

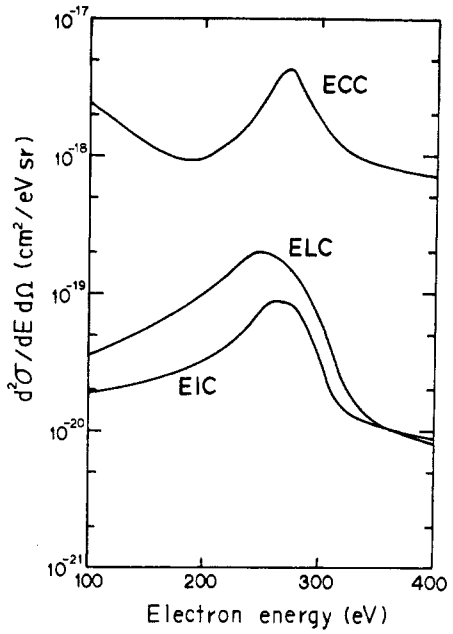

Figure 3. Doubly differential cross section for free electron production at $2° \pm 2°$ ejection angle in the region of the cusp comparing the yield of target electrons (denoted as ECC), projectile electrons (denoted as ELC) and their EIC component, for 10 MeV F^{6+} colliding with Ne. The statistical uncertainties of the cross sections are less than 20%.

the cusp electron originated from the target and was produced by ECC. Likewise, if the projectile was found to be stripped, the cusp was attributed to projectile electron and ELC. Thus, due to interchange, an electron that is considered to be an ECC electron may not have originated in the target, or, similarly, what is termed an ELC electron may not have come from the projectile.

To try to illustrate the implications of this suggestion we have used the present IEM treatment to calculate the doubly differential cross section for free electron production at an ejection angle of 2° in the vicinity of the cusp. Since in the present model the electrons are distinguishable, we have partitioned the electronic spectra into components representing the contributions from the yield of target and projectile electrons, the results of which are displayed in figure 3 for 10 MeV F^{6+} impact of Ne. In the figure we have indicated the yield of target electrons as ECC, the yield of projectile electrons as ELC and the yield of electrons which originate from either projectile or target through the interchange process as EIC. This latter mechanism we have termed 'electron interchange to the continuum' (EIC) for short, by simple analogy. We note that these definitions of ECC and ELC differ from the usual experimental definition of these processes since, for example, the measurement of an electron in coincidence with an outgoing ionized projectile does not guarantee that the cusp electron originated in the projectile.

In this case, since the projectile electron is rather tightly bound, the yield of target electrons dominates. Thus the total cusp which would be measured is predominantly composed of ECC electrons. We find that EIC turns out to be quite small relative to the total yield of target electrons, but is comparable with that of projectile electrons. The probability of interchange should increase for other systems where the target and projectile electrons have more symmetrical binding energies and the collision velocity is lower and, therefore, the EIC contribution could be a large component of the measured cusp.

5. Summary

The present work provides a new theoretical technique to predict and aid in analysing coincident charge state production cross sections by explicitly including an interacting projectile electron in an n-active electron model. It is found that this model allows a more realistic representation of electron stripping from the projectile. Further, the conventional IEM has been shown to be inadequate in accurately predicting the simultaneous values of the projectile and target charge states after the collision. Specifically, this failure is mainly attributable to the improper account of the sequential ionization potentials of the target.

In addition, we find that the conventional experimental separation of the cusp into its ECC and ELC components may be complicated in many-electron systems since the measurement of an electron in coincidence with the projectile charge state is not sufficient to determine whether the electron originated in the target or the projectile. For example, an electron interchange between target and projectile would leave the projectile charge unchanged and would be experimentally attributed to ECC. However, the yield of electrons associated with this type of measurement is composed of both target electrons captured to the continuum of the projectile and projectile electrons lost to its continuum. Finally, we recognize that, due to the indistinguishability of the projectile and target electrons, the experimental separation of ECC and ELC is not

feasible when EIC is a significant contribution. However, interchange should be accounted for in other theoretical treatments which investigate cusp electron production.

Acknowledgments

The authors would like to acknowledge the support of the Office of Fusion Energy, US Department of Energy.

References

Abrines R and Percival I C 1966 *Proc. R. Soc.* **88** 861
Cocke C L 1979 *Phys. Rev.* A **20** 749
Datz S, Hippler R, Andersen L H, Dittner P F, Knudsen H, Krause H F, Miller P D, Pepmiller P L, Rosseel T, Schuch R, Stolterfoht N, Yamazaki Y and Vane C R 1990 *Phys. Rev.* A **41** 3559
Freyou J, Breinig M, Gaither C C III and Underwood T A 1990 *Phys. Rev.* A **41** 1315
Gray T J, Cocke C L and Justiniano E 1980 *Phys. Rev.* A **22** 849
Kelbch S, Cocke C L, Hagmann S, Horbatsch M, Kelbch C, Koch R and Schmidt-Böcking H 1988 *Phys. Lett.* **127** 92
Kelbch S, Cocke C L, Hagmann S, Horbatsch M, Kelbch C, Koch R, Schmidt-Böcking H and Ullrich J 1990 *J. Phys. B: At. Mol. Opt. Phys.* **23** 1277
Kelbch S, Ullrich J, Mann R, Richard P and Schmidt-Böcking H 1985 *J. Phys. B: At. Mol. Phys.* **18** 323
McGuire J H and Weaver L 1977 *Phys. Rev.* A **16** 41
Müller A, Schuch B, Groh W, Salzborn E, Beyer H F, Mokler P H and Olson R E 1986 *Phys. Rev.* A **33** 3010
Olson R E 1988 *Electronic and Atomic Collisions* ed H B Gilbody, W R Newell, F H Read and A C H Smith (Amsterdam: North-Holland) p 271
Olson R E, Ullrich J and Schmidt-Böcking H 1987 *J. Phys. B: At. Mol. Phys.* **20** L809
—— 1989 *Phys. Rev.* A **39** 5572
Reinhold C O, Schultz D R, Olson R E, Toburen L H and DuBois R D 1990 *J. Phys. B: At. Mol. Opt. Phys.* **23** L297
Schlachter A S, Groh W, Müller A, Beyer H F, Mann R and Olson R E 1982 *Phys. Rev.* A **26** 1373
Schuch R, Schöne H, Miller P D, Krause H F, Dittner P F, Datz S and Olson R E 1988 *Phys. Rev. Lett.* **60** 925
Tawara T, Tonuma T, Kumagi H and Matsuo T 1990 *Phys. Rev.* A **41** 116
Ullrich J, Bethege K, Kelbch S, Schadt W, Schmidt-Böcking H and Stieberg K E 1986 *J. Phys. B: At. Mol. Phys.* **19** 448